

## SPACEBORNE RADAR MONITORING OF SOIL FREEZING/THAWING PROCESSES IN THE ARCTIC TUNDRA

V. L. Mironov and K. V. Muzalevsky

UDC 537.86; 550.35

In this article, the possibility of measuring the average temperature in the active topsoil of the Arctic tundra from the temperature dependence of the radar backscattering coefficient is theoretically studied. The radar backscattering coefficient is simulated by the small perturbation method at a frequency of 1.26 GHz of radars placed onboard ALOS-2 and SMAP satellites. In simulation, the soil density, surface roughness, and temperature and moisture profiles measured *in situ* at the biosphere station Franklin Bluffs, Alaska ( $69^{\circ}39'N$ ,  $148^{\circ}43'W$ ), from August 1, 2000 to July 1, 2001 were used. The soil permittivity was calculated for the generalized temperature-dependent refractive mixing dielectric model for organic rich soil whose sample was taken on the Alaska North Slope ( $68^{\circ}38'N$ ,  $149^{\circ}35'W$ ). This model allows the complex dielectric constant of moist thawed and frozen soil to be calculated at temperatures in the range from  $-30^{\circ}C$  to  $+25^{\circ}C$ . It is demonstrated that the radar backscattering coefficient is correlated with the topsoil temperature with the error less than  $5.7^{\circ}C$  during the entire period of freezing and thawing.

**Keywords:** radar backscattering coefficient, soil temperature, active topsoil, freezing/thawing soil, complex dielectric constant, Arctic tundra.

### INTRODUCTION

Temperature of the active topsoil of the Arctic tundra is a main indicator that characterizes the intensity of carbon dioxide and methane emissions into the atmosphere as well as the processes of the heat and moisture exchange between the atmosphere and the active topsoil which most dynamically follow the climate changes [1]. The most comprehensive results of remote sensing of the soil temperature of the Arctic tundra obtained using C-band radars RADARSAT-1 and ASCAT were discussed in [2] and [3], respectively. In [2], a regression model between the agricultural soil surface temperature and the radar backscattering coefficient was developed to classify RADARSAT-1 images of frozen or thawed topsoil under dry snow cover. A noticeable correlation was observed between the topsoil state (frozen/thawed) and the soil temperature at a depth of 5 cm [2]. In [3], based on the behavior of time series of the radar backscattering coefficient versus the soil temperature at a depth of 7 cm, frozen and unfrozen conditions were distinguished by using the logistic curve with a threshold temperature of  $0^{\circ}C$ . Though Naeimi *et al.* [3] noted that during the freezing/thawing transition period the terms *frozen* and *thawed* could be misleading, because different soil layers may be in different states.

In contrast to [2] and [3], the present work is aimed at the development of an algorithm for measuring the temperature in the active frozen topsoil of the Arctic tundra based on the radar backscattering coefficient data of future L-band ALOS-2 and SMAP satellites. As a first phase of these studies, we consider the bare soil without vegetation and snow cover because, according to [4], the effects of dry snow scattering and attenuation can be neglected for the L-band. We consider the case of vertical polarization that turns out to be most sensitive to variations in the soil temperature.

---

<sup>1</sup>L. V. Kirensky Institute of Physics of the Siberian Branch of the Russian Academy of Sciences, Krasnoyarsk, Russia; <sup>2</sup>M. F. Reshetnev Siberian State Aerospace University, Krasnoyarsk, Russia, e-mail: rsdvm@ksc.krasn.ru; rsdkm@ksc.krasn.ru. Translated from Izvestiya Vysshikh Uchebnykh Zavedenii, Fizika, No. 8, pp. 40–43, August, 2012. Original article submitted June 15, 2012.

## MODELING OF THE RADAR BACKSCATTERING COEFFICIENT

In the approximation of small perturbations method (the average height of surface roughness is much smaller than the radiation wavelength), the radar backscattering coefficient for vertical polarization can be estimated from the following formula [5]:

$$\begin{aligned}\sigma_{VV}(\theta) &= 8k_0^4\sigma_1^2 \cos^4 \theta |\alpha_{VV}|^2 K(2k_0 \sin \theta), \\ \alpha_{VV} &= R_V(\theta, \varepsilon(T(z), W, f)) + [1 + R_V(\theta, \varepsilon(T(z), W, f))]^2 \frac{(\varepsilon_s - 1)}{\varepsilon_s} \tan^2 \theta.\end{aligned}\quad (1)$$

where  $R_V(\theta, \varepsilon(T(z), W, f))$  is the Fresnel reflection coefficient calculated for a layered medium by the iterative algorithm presented in [6],  $\theta$  is the incidence angle,  $\varepsilon(T(z), W, f)$  is the relative complex permittivity of soil,  $T(z)$  is the temperature of the soil at depth  $z$ ,  $W$  is the volumetric soil water content,  $f = 1.26$  GHz is the wave frequency,  $\varepsilon_s = \varepsilon(T(z = 0), W, f)$  is the dielectric permittivity of the topsoil,  $\sigma_1$  is the standard deviation of surface roughness heights,  $K(2k_0 \sin \theta)$  is the spectral density of surface roughness heights.

For the exponential correlation function of the surface roughness heights, the spectral density of distribution of surface roughness heights is given by the formula

$$K(2k_0 \sin \theta) = l^2 [1 + (2k_0 l \sin \theta)^2]^{-1.5}, \quad (2)$$

where  $l$  is the correlation length.

Radar backscattering coefficient (1) was calculated from the temperature profiles measured in [7] to depths of 1 m of the tundra soil in the Franklin Bluffs, Alaska ( $69^{\circ}39'N$ ,  $148^{\circ}43'W$ ) from August 1, 2000 to July 1, 2001. The relative complex permittivity of the organic rich soil sampled in the North Slope, Alaska ( $68^{\circ}38'N$ ,  $149^{\circ}35'W$ ) was calculated at temperatures in the range from  $-30^{\circ}C$  to  $25^{\circ}C$  for the temperature-dependent generalized refractive mixing dielectric model (TD GRMDM) [8]. This soil comprised about 87% organic matter, 8% quartz, and 5% calcite. The relative complex permittivity of the soil was calculated for typical density values of  $0.3 \text{ g/cm}^3$  and bulk topsoil layer moisture of 40%. We note that the model [8] was constructed for soil samples in the process of freezing.

## METHOD OF RETRIEVAL OF THE SOIL TEMPERATURE

The method is intended for future ALOS-2 and SMAP satellites and sensing angle of  $40^{\circ}$ . As follows from specification of radars to be placed onboard the ALOS-2 and SMAP satellites [9], the accuracy of measuring the radar backscattering coefficient will not exceed 1 dB. Therefore, the random noise component distributed by the Gaussian law with half-width of 1 dB was added to the radar backscattering coefficient calculated from formulas (1) and (2). Similar to [10], we characterize the soil cover state by the surface state factor (SSF)

$$\text{SSF} = \frac{1}{2} + \frac{\sigma_V(t) - \sigma_V^{\text{Summer}}}{\sigma_V^{\text{Summer}} - \sigma_V^{\text{Winter}}}, \quad (3)$$

where  $\sigma_V^{\text{Summer}}$  and  $\sigma_V^{\text{Winter}}$  are the mean values of radar backscattering coefficient in summer and winter, respectively,  $\sigma_V(t)$  is the running value of the radar backscattering coefficient, and  $t$  is time. The results of SSF simulation using formulas (1)–(3) are shown in Fig. 1 together with the seasonal cycles of the mean temperature of 5-cm topsoil layer. Figure 2 shows the soil temperatures at depths of 0, 2.5, and 5 cm, respectively. The time series of the SSF and soil temperature were smoothed over a ten day period.

As can be seen from Fig. 1, the seasonal SSF variations are highly correlated with the seasonal variations of the soil temperature, taking negative values at temperatures below  $0^{\circ}C$ . Consequently, we can classify a 5-cm thick topsoil

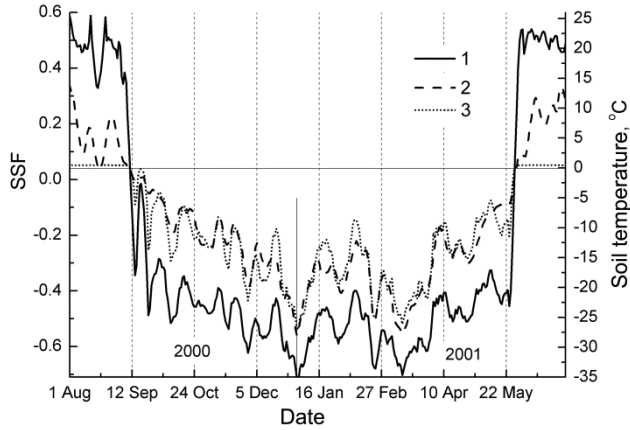


Fig. 1

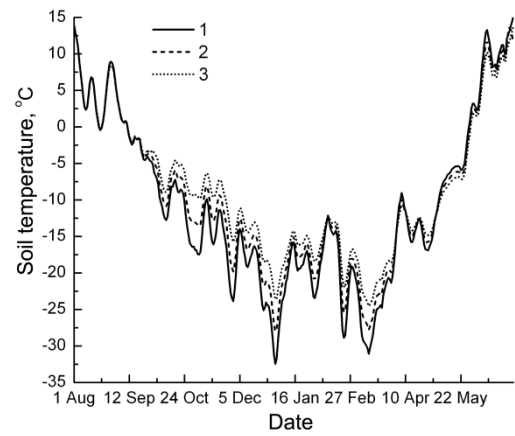


Fig. 2

Fig. 1. Seasonal cycles of SSF with vertical polarization (curve 1), mean topsoil temperature in the active layer with a thickness of 5cm (curve 2), and retrieved soil temperature (curve 3).

Fig. 2. Seasonal cycles of the soil temperature at depths of 0 (curve 1), 2.5 (curve 2), and 5 cm (curve 3).

of the Arctic tundra as frozen when the SSF measured by the radar takes negative values. This result is in good agreement with the classification performed in [11] based on the radar backscattering coefficient measured over some territories of the Alaska tundra.

In contrast to [10] and [11], results of simulations performed in this paper demonstrated that not only the frozen/thawed state, but also the temperature of the 5-cm thick topsoil layer can be determined from the measured radar backscattering coefficient. For this purpose, we suggested the calibration function for the SSF as a function of the temperature in the form of the Boltzmann function

$$T_{sp} = T_0 + \frac{\Delta T}{\frac{SSF - SSF_0}{\Delta SSF}}, \quad (4)$$

where  $-0.75 \leq SSF \leq 0.4$ ,  $T_0 = 0.47 \pm 0.47^\circ\text{C}$ ,  $\Delta T = -33.6 \pm 2.2^\circ\text{C}$ ,  $SSF_0 = -0.53 \pm 0.02$ , and  $\Delta SSF = 0.13 \pm 0.01$ . This function is shown by the solid curve in Fig. 3. Using calibration curve (4) and SSFs measured in winter, we determined the soil temperatures (see curve 3 in Fig. 1). The correlation of the soil temperature determined by this method (see curve 3 in Fig. 1) with the mean soil temperature measured *in situ* in the test site (see curve 2 in Fig. 1) is presented in Fig. 4.

As can be seen from the correlation analysis of the data shown in Fig. 4, the soil temperature retrieved from the measured SSF values deviates from the true soil temperature by about  $5.7^\circ\text{C}$ . This error is comparable with the error in measuring the temperature of the frozen soil with the AMSR-E radiometer [12].

## CONCLUSIONS

In this article, the possibility of retrieval of the temperature in the active topsoil of the Arctic tundra from L-band radar data has been studied. It was demonstrated that the surface state factor introduced in [10] and [11] allowed one not only to identify the frozen and thawed soil states, but also to determine the mean temperature of the 5-cm thick topsoil frozen layer with an error of  $5.7^\circ\text{C}$ . The proposed method is specifically intended for retrieving the temperature

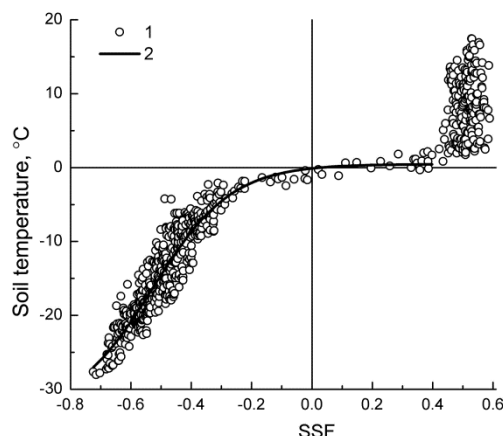


Fig. 3

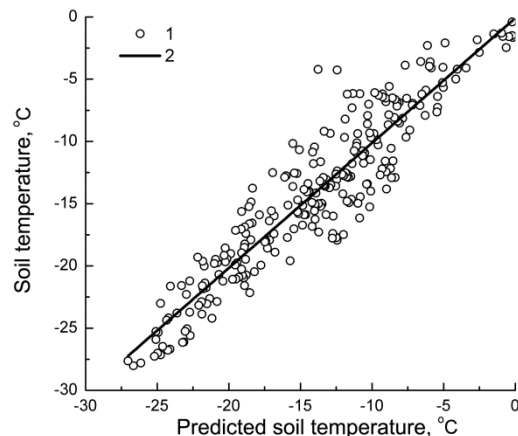


Fig. 4

Fig. 3. Temperature dependence of SSF (1) measured from August 1, 2000 to July 1, 2001 (open circles) and solid calibration curve 2 calculated from formula (4).

Fig. 4. Correlation (1) of the predicted soil temperature,  $T_{sp}$ , with the mean soil temperature,  $T_s$ , in the active layer with a thickness of 5 cm. The linear fit is expressed as follows:  $T_s = -(0.08 \pm 0.37) + (1.01 \pm 0.03) \cdot T_{sp}$ , the squared correlation coefficients,  $R^2$ , and the root mean square error (RMSE) are equal to 0.87 and 5.7°C, respectively.

of frozen soil and mapping the territories with permafrost degradation in the Arctic region from the data of the ALOS-2 and SMAP satellites.

## REFERENCES

1. K. Schaefer, T. Zhang, L. Bruhwiler, and A. Barrett, Tellus, No. 63B, 165–180 (2011).
2. J. Khaldoune, É. van Bochove, M. Bernier, and M. S. Nolin, Appl. Envir. Soil Science, ID193237-1–16 (2011).
3. V. Naeimi, C. Paulik, A. Bartsch, *et al.*, IEEE Trans. Geosci. Remote Sens., **50**, No. 7, 2566–2582.
4. Z. Li, H. Guo, and J. Shi, Proc. Geoscience and Remote Sensing Symposium, Vol. 4, 1757–1759 (2000).
5. S. A. Komarov and V. L. Mironov, Microwave Remote Sensing of Soils [in Russian], Publishing House of the Siberian Branch of the Russian Academy of Sciences, Novosibirsk (2000).
6. L. M. Brekhovskikh, Waves in Layered Media [in Russian], Nauka, Moscow (1957).
7. Alaska Geobotany Center: Biocomplexity of Forest Boil Ecosystems [PDF]. Database (2001), <http://www.geobotany.uaf.edu/cryoturbation/project/frbluffs/>.
8. V. L. Mironov, R. D. de Roo, and I. V. Savin, IEEE Trans. Geosci. Remote Sens., **48**, No. 6, 2544–2556 (2010).
9. Soil Moisture Active and Passive (SMAP) [PDF] (2012), <http://smap.jpl.nasa.gov/>.
10. Y. Kim, J. S. Kimball, K. S. McDonald, and J. Glassy, IEEE Trans. Geosci. Remote Sens., **49**, No. 3, 949–960 (2011).
11. A. Colliander, K. McDonald, R. Zimmermann, *et al.*, IEEE Trans. Geosci. Remote Sens., **50**, No. 2, 461–468 (2012).
12. L. A. Jones, J. S. Kimball, K. C. McDonald, *et al.*, IEEE Trans. Geosci. Remote Sens., **45**, 2004–2018 (2007).